

The Spatial Blindspot of Vision-Language Models

Nahid Alam^{1,†}, Leema Krishna Murali^{1,5,†}, Siddhant Bharadwaj², Patrick Liu^{3,†}, Timothy Chung^{4,1}, Drishti Sharma¹, Akshata A.^{1,†}, Kranthi Kiran^{1,6}, Wesley Tam^{6,†}, Bala Krishna S Vigesna⁷,

¹Cohere Labs Community, ²Indian Institute of Science, Bangalore, ³UIUC,
⁴Imperial College London, ⁵Eisai Inc., ⁶EleutherAI, ⁷Georgia Institute of Technology

† Work done as part of the EleutherAI SOAR Program

nahid.m.alam@gmail.com

Abstract

Vision-language models (VLMs) have advanced rapidly, but their ability to capture spatial relationships remains a blindspot. Current VLMs are typically built with contrastive language-image pretraining (CLIP) style image encoders. The training recipe often flattens images into 1D patch sequences, discarding the 2D structure necessary for spatial reasoning. We argue that this lack of spatial awareness is a missing dimension in VLM design and a bottleneck for applications requiring spatial grounding, such as robotics and embodied AI. To address this, we investigate (i) image encoders trained with alternative objectives and (ii) 2D positional encodings. Our experiments show that these architectural choices can lead to improved spatial reasoning on several benchmarks.

1. Introduction

Vision–language models (VLMs) have achieved impressive results in recognition, captioning, and visual question answering, yet their ability to reason about space remains fragile. Although spatial structure is fundamental to visual perception, most VLMs treat images primarily as sources of semantic tokens, rather than as organized physical layouts. This limits their reliability in tasks requiring geometric reasoning, precise localization, and spatial interaction.

A source of this weakness lies in the visual foundations of modern VLMs. They rely on large, pre-trained image encoders [13, 30, 33, 36], typically frozen or lightly adapted [2, 16, 21, 24], that are optimized for global semantic alignment. Prior work shows that CLIP-style models emphasize overall semantics over local structure [39] and exhibit poor robustness to simple geometric transformations [3].

While recent efforts explore alternative pretraining objectives [14, 26, 39, 40], their impact on spatial reasoning within VLMs remains underexplored.

Spatial information is further degraded during vision–language alignment. Most existing VLMs flatten visual tokens into a 1D sequence and apply RoPE-1D [35], a design choice that has been shown to weaken spatial awareness [45, 46]. Qwen2-VL [42] shows that explicitly factorizing positional encoding along spatial axes can improve structural preservation. Their findings suggest that alignment design is an area worth exploring for spatial understanding.

Foundational VLMs [2, 21, 24, 43] are rarely evaluated on benchmarks that directly probe spatial reasoning. Standard evaluations emphasize semantic competence, offering limited insight into models’ understanding of geometry, relative position, and the scene layout.

In this work, we treat spatial grounding as a first-class design axis in VLMs and make the following contributions:

1. We evaluate state-of-the-art VLMs on spatial reasoning benchmarks and identify gaps between semantic competence and spatial understanding.
2. We study alternative image encoders—SigLIP, SigLIP2, and AIMv2—within the LLaVA framework and quantify how encoder choice affects spatial reasoning.
3. We use 2D-RoPE for vision–language alignment to preserve the image’s 2D structure and improve spatial reasoning performance on several benchmarks.

2. Related Work

2.1. Image Encoders

In recent years, we have seen progress on image encoders aligned with their own text captioning. CLIP [33] aligns image and text representations through a large-scale contrastive loss on paired dataset, and demonstrates strong

zero-shot generalization across classification and retrieval tasks. In contrast, DINOv2 [30] is a visual model trained with a self-supervised masked image modeling objective. This allows DINOv2 to learn rich, pixel-level features by predicting masked-out image patches, without relying on paired text supervision. BLIP [20] proposed a unified framework that integrates both contrastive pre-training for vision and generative objectives such as image–text matching and captioning. BLIP demonstrated that combining discriminative and generative signals leads to richer cross-modal representations and improved downstream transfer. BLIP-2 [21] further advanced this line by introducing a lightweight querying transformer that bridges frozen image encoders with large language models, enabling efficient vision–language alignment without end-to-end pretraining of massive multimodal models. SigLIP [44] improves CLIP by replacing the softmax contrastive loss with a pairwise sigmoid loss, removing batch-size dependencies and resulting in more stable training dynamics and efficient scaling. SigLIP2 [40] extends this line of work by augmenting the SigLIP training recipe with self-distillation and masked prediction objectives, resulting in higher-quality dense features, and improved localization across vision–language benchmarks. SigLIP2 also introduces the NaFlex variant, which preserves native aspect ratios and supports variable sequence lengths. The NaFlex variant provides empirical gains on aspect-sensitive tasks such as OCR and document understanding. In contrast to these contrastive and bridging approaches, AIMv2 [14] introduces an autoregressive multimodal pretraining framework that unifies vision and language by pairing a vision encoder with a decoder trained to jointly generate image patches and text tokens. Cocchi et al. [10] conduct a study that systematically pairs various LLMs with different visual backbones such as CLIP, DINOv2, SigLIP, and SigLIP2 to understand the strengths and limitations of various VLM integration strategies. Our work differs from theirs as we focus on spatial awareness along with the integration of M-RoPE in image encoders; specifically 2D-RoPE for images.

2.2. Spatial Reasoning

Zhang et al. [45] classified spatial reasoning into two categories, static vs. dynamic. Static spatial reasoning refers to understanding spatial relationships in fixed configurations, where objects do not change positions over time. These tasks test whether a model can identify, compare, or infer spatial arrangements from still images or single states of a scene. For example, determining whether ‘the book is to the left of the laptop’ or ‘the chair is behind the table’ requires recognizing and reasoning about stable relative positions. Static reasoning often emphasizes relational concepts such as distance, orientation, containment, or perspective, without involving temporal changes. Dynamic spatial

reasoning, on the other hand, involves scenarios in which the spatial configuration evolves. Here, models must account for motion, transformation, or sequential changes in a scene. Typical examples include predicting the outcome of an object’s movement, tracking shifting perspectives, or reasoning about cause-and-effect actions in space. Unlike static reasoning, dynamic tasks demand temporal and often causal understanding, requiring models to build an implicit representation of change and transformation. Another way to categorize spatial reasoning is 2D vs. 3D images. 2D reasoning focuses on relationships within 2D images, such as relative position, alignment, or counting, whereas 3D reasoning requires understanding depth, perspective, and volumetric relations. In this paper, we focus on static spatial awareness in 2D images.

2.3. VLMs and Spatial Awareness

Recent advances in LLMs and general purpose image encoders, such as CLIP [33] and SigLIP [44] have significantly improved VLM capabilities. Architectures such as Flamingo [2], LLaVA [23, 24], KOSMOS [31, 32], Florence-2 [43], and Molmo [12] demonstrate strong performance in tasks such as image captioning, visual question answering (VQA) and complex reasoning. Qwen2-VL [42] introduced multimodal rotary position encoding (M-RoPE) and dynamic resolution techniques, while PaLI’s joint modality scaling and cross-lingual learning [7, 8] have improved vision-language understanding. These VLMs tend to rely on implicit visual features learned during training rather than explicitly structured representations of spatial information needed for world understanding. RoboSpatial [34] is an annotated dataset specifically designed for spatial understanding in VLMs that includes 1 million images, 5,000 3D scans, and 3 million annotated spatial relationships. The pairing of 2D egocentric images with 3D scans in RoboSpatial makes it suitable for both 2D and 3D spatial understanding tasks. SpatialVLM [6] focuses on training VLMs with spatial reasoning dataset on the internet to improve their 3D spatial understanding. This framework enhances the ability of VLMs to recognize quantitative relationships between physical objects, such as distances and size differences, which are crucial for many real-world tasks. SpatialVLM has also shown potential in robotics as a tool for providing fine-grained reward annotations. MM-Spatial [11] introduces CA-VQA, a new supervised fine-tuning dataset and benchmark focused on indoor scenes. It targets tasks such as spatial relationship reasoning, metric estimation, and 3D grounding. By training MM-Spatial on CA-VQA, the model achieves state-of-the-art performance in 3D spatial understanding, highlighting the value of incorporating depth and multiview cues. SpatialRGPT [9] introduces a data curation pipeline that enables effective learning of regional representations from 3D

scene graphs. It also features a flexible plugin module for integrating depth information into the visual encoder of existing VLMs. This allows SpatialRGPT to accurately perceive the relative directions and distances of user-specified regions within a visual scene.

2.4. Measuring Spatial Awareness

There are a number of benchmarks evaluating VLMs on spatial awareness; spanning across tasks such as 2D layout understanding, 3D geometric reasoning, counting, and relational question answering. Multimodal Visual Pattern (MMVP) benchmark [39] is a set of 300 images in 9 categories, designed by observing CLIP-blind pairs. CV-Bench [38] includes both the 2D and 3D tasks around spatial relationships, object counting, depth ordering, and relative distance estimation. GQA [15] leverages scene graph annotations and functional programs to generate compositional questions, and includes subsets like compare, verify, and logical that specifically test spatial relations such as left, right, on, and under. Visual Spatial Reasoning (VSR) [22] assesses fine-grained relational understanding through 66 annotated spatial relations in natural images, while TopViewRS [19] measures reasoning over semantic top-view maps. TallyQA [1] and CountBenchQA [5] address object numerosity under occlusion and clutter.

3. Experimental Setup

3.1. Methods

Our experiment is based on the LLaVA [24] framework as shown in Figure 1. To explore spatial awareness in VLMs, we extend the LLaVA architecture by integrating alternative image encoders beyond CLIP along with 2D-RoPE to preserve the inherent 2D spatial structure as shown in Figure 2. Specifically, we experiment with CLIP, SigLIP, SigLIP2, AIMv2 along with a modified design to include 2D-RoPE. Our hypothesis is that these encoder designs will better capture hierarchical spatial cues and contextual relationships across image regions. Unlike standard RoPE, 2D-RoPE encodes both horizontal and vertical patch indices through concatenated sinusoidal embeddings, providing explicit spatial priors for attention. In our implementation, 2D-RoPE is applied after patch embeddings are projected into query and key vectors, ensuring that spatial relations are injected directly into the attention mechanism rather than at the raw patch level. We hypothesize that these design choices will build a VLM with better relative position understanding in 2D images.

3.2. Training Strategies

We train our models in two stages: pretraining and instruction fine-tuning. The training process uses the same dataset used in LLaVA pretraining and instruction tuning respec-

tively. For each image X_v , we used the single-turn conversation data

$$(X_q^1, X_a^1, \dots, X_q^T, X_a^T)$$

where T is the total number of turns from LLaVA.

We conduct our experiments using a cluster of 8 NVIDIA A40 GPUs, each with 48 GB of VRAM. For both pretraining and fine-tuning, we resize input images to a resolution of 256×256 pixels.

The pretraining process focuses solely on training the projection matrix. We use a per-device batch size of 32, which results in a global batch size of 256. We optimize the model using the AdamW optimizer with a learning rate of 1e-3, and a cosine learning rate scheduler is applied. For fine-tuning, we perform a full model update. The fine-tuning configuration uses a learning rate of 2e-5, per-device batch size of 16, resulting in a global batch size of 128.

4. Results

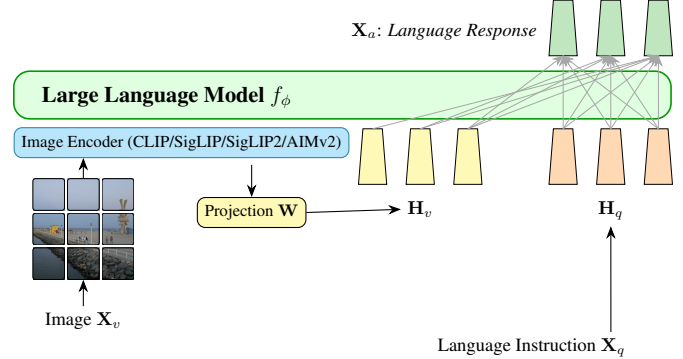


Figure 1. Our experimental approach with LLaVA Framework [24] that compares the performance of different image encoders and 2D-RoPE variants.

We compare frontier models and LLaVA variants on various benchmarks. Our work is based on the LLaVA-1.5 7B model. Therefore, all encoders and their 2D-RoPE variants that we trained are 7B models. Frontier models between the 2B to 8B parameter range were compared with the LLaVA variants we trained. For comparison purposes, we used LLaVA-NeXT 7B [25], LLaVA-OneVision-qwen2-7B-ov-hf [18], Qwen2.5-VL-8B [4], SmoVLM2-2.2B-Instruct [27], Gemma3-4b-it [37], PaliGemma2-3b-mix-448 [5] and Molmo-7B-D-0924 [12].

4.1. Evaluating on General Purpose Benchmarks

As shown in Table 1, Qwen2.5-VL achieves the strongest overall performance, obtaining the highest scores on MMMU_Val, MME, CCBench, and SEEDBench-IMG. Among the LLaVA variants, AIMv2 demonstrates the most consistent results, particularly on MME and SEEDBench-IMG, although its 2D-RoPE counterpart provides only

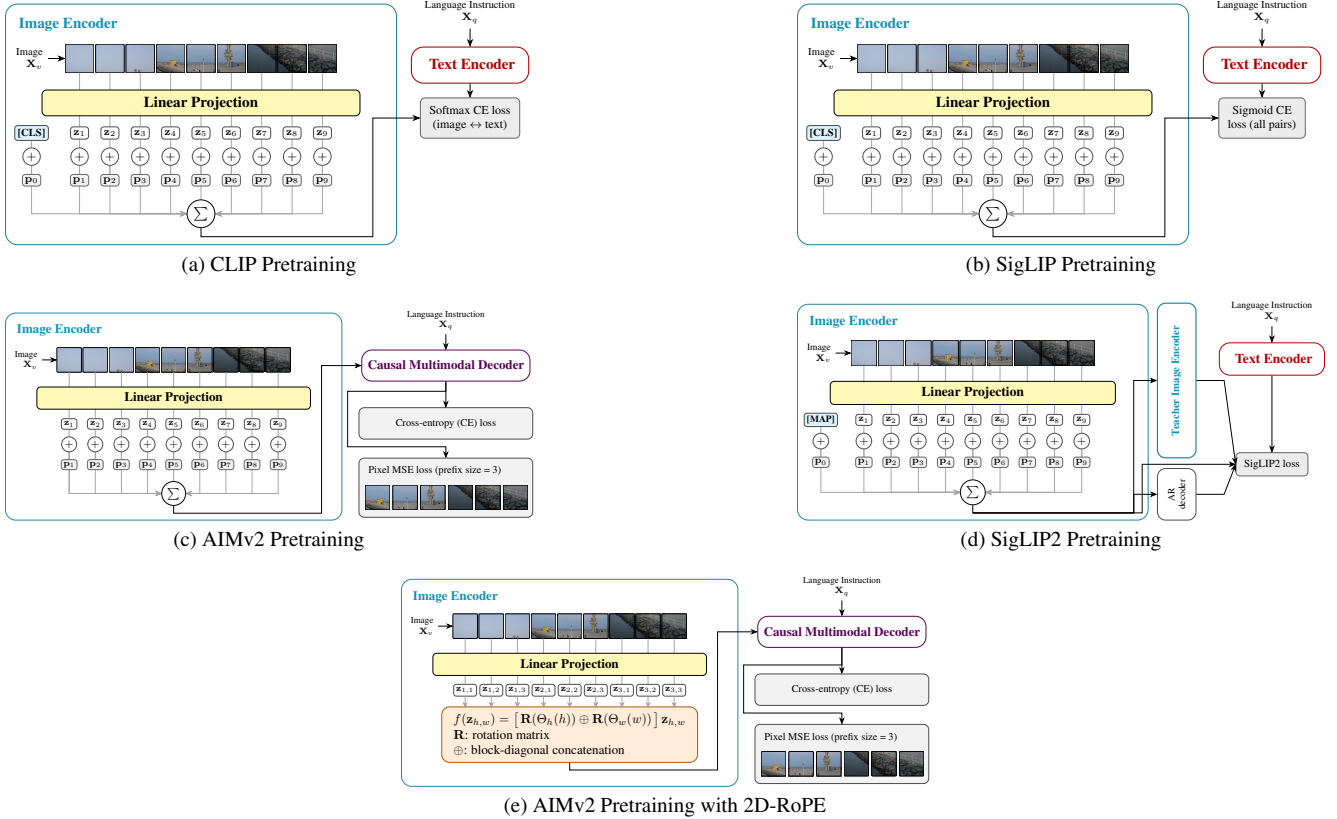


Figure 2. Pretraining strategies with various image backbones and 2D-RoPE

Table 1. Comparison of multimodal models across MMMU_Val, MME, CCBench, and SEEDBench-IMG. Values underlined indicate the best-performing model overall, while values in **bold** highlight the best-performing LLaVA encoder variant in each benchmark.

Models	MMMU_Val	MME	CCBench	SEEDBench-IMG
Qwen2.5-VL	<u>0.580</u>	0.826	<u>0.592</u>	0.770
LLaVA-NeXT	0.376	0.632	0.243	0.696
LLaVA-OneVision	0.479	0.712	0.549	0.767
SmolVLM2	0.416	0.640	0.231	0.713
Gemma3-4b-it	0.473	0.620	0.369	0.655
PaliGemma	0.307	0.580	0.333	0.715
Molmo	0.491	0.662	0.367	0.746
LLaVA-1.5	0.322	0.589	0.084	0.601
LLaVA-2D-RoPE	0.298	0.582	0.086	0.585
LLaVA-SigLIP	0.303	0.559	0.071	0.567
LLaVA-SigLIP-2D-RoPE	0.334	0.525	0.080	0.545
LLaVA-SigLIP2	0.309	0.495	0.086	0.548
LLaVA-SigLIP2-2D-RoPE	0.323	0.542	0.086	0.527
LLaVA-AIMv2	0.314	0.573	0.086	0.595
LLaVA-AIMv2-2D-RoPE	0.311	0.563	0.114	0.586

marginal gains on certain metrics and about 1.75% drop in MME. The effect of 2D-RoPE is mixed across variants. For example, LLaVA-SigLIP improves about 10%

on MMMU_Val, while other models show little benefit or even reduced performance. LLaVA-SigLIP-2D-RoPE achieves the strongest MMMU_Val score among LLaVA

Table 2. Comparison of frontier models and LLaVA variants across spatial understanding benchmarks. Values underlined indicate the best-performing frontier model; values in **bold** indicate the best-performing LLaVA variant.

Models	MMVP	CV-Bench 2D Overall	TallyQA	GQA Overall	VSR	Top- ViewRS	Count- BenchQA
LLaVA-NeXT	0.667	0.606	0.733	<u>63.786</u>	63.994	0.409	0.515
LLaVA-OneVision	0.767	0.730	0.797	62.140	<u>77.741</u>	0.414	0.823
Qwen2.5-VL	<u>0.770</u>	<u>0.754</u>	0.800	60.391	<u>89.116</u>	<u>0.456</u>	<u>0.891</u>
SmolVLM2	0.687	0.577	0.729	50.574	71.277	0.416	0.692
Gemma3-4b-it	0.708	0.659	0.525	31.277	55.074	0.334	0.713
PaliGemma	0.667	0.624	0.794	62.570	65.139	0.322	0.674
Molmo	0.753	0.728	<u>0.808</u>	55.295	76.432	0.323	0.858
LLaVA v1.5	0.577	0.490	0.707	33.225	55.810	0.384	0.468
LLaVA-2D-RoPE	0.513	0.443	0.654	34.433	57.201	0.283	0.290
LLaVA-SigLIP	0.433	0.412	0.672	25.648	54.910	0.349	0.581
LLaVA-SigLIP-2D-RoPE	0.507	0.425	0.616	38.448	57.692	0.295	0.483
LLaVA-SigLIP2	0.427	0.442	0.684	23.970	52.701	0.371	0.532
LLaVA-SigLIP2-2D-RoPE	0.480	0.415	0.646	34.560	56.465	0.330	0.402
LLaVA-AIMv2	0.513	0.466	0.710	32.541	56.219	0.339	0.739
LLaVA-AIMv2-2D-RoPE	0.560	0.432	0.690	32.342	60.311	0.338	0.719

encoders, but AIMv2 remains more competitive across multiple benchmarks.

4.2. Evaluating on Spatial Benchmarks

In Table 2, Qwen2.5-VL stands out as the strongest frontier model overall, achieving the highest performance on CV-Bench 2D, MMVP, VSR, TopViewRS, and CountBenchQA. LLaVA-NeXT leads frontier models on GQA Overall, while Molmo achieves the best TallyQA score among frontiers, indicating complementary strengths across different tasks. Among the LLaVA variants, performance is more fragmented: LLaVA-AIMv2 shows the most consistent improvements, reaching the highest scores on CV-Bench 2D, TallyQA, and CountBenchQA. LLaVA-AIMv2-2D-RoPE improves MMVP and leads on VSR. LLaVA-SigLIP-2D-RoPE dominates GQA Overall, and LLaVA-SigLIP2 leads in TopViewRS. We observe that although the LLaVA variants surpass Gemma3-4b-it in TallyQA, VSR; their overall performance did not surpass other frontier models. We think this is because of how Gemma3-4b-it is designed. Gemma3-4b-it uses SigLIP variant as its vision encoder, but the fixed resolution of the encoder with Pan & Scan algorithm. Pan & Scan is a preprocessing algorithm that allows the model to handle high-resolution and non-square images by breaking them down into smaller, fixed-size crops. This is necessary because Gemma 3’s vision encoder can only process images at a fixed resolution of 896x896 pixels. This design leads to information loss that hinders performance in benchmarks that require fine-grained visual reasoning, such as VSR and TallyQA. In Table 3, we observe that Gemma3-4b-it mistakenly thinks that

the chopsticks are on the left side of the ramen bowl - reconfirming our hypothesis.

In Table 2, we also observe improved performance using AIMv2 encoder and its 2D-RoPE version over other vision encoders in the LLaVA framework. AIMv2 design focuses on the image-first principle, where the model is trained to process all the image patches before decoding the text tokens in an autoregressive manner. This dense per-token supervision helps with tasks requiring fine-grained perception, such as in MMVP, CV-Bench, TallyQA, CountBenchQA, and VSR. We also believe that the two-stage captioning pipeline to generate AIMv2 training data helps in count-related examples, causing the LLaVA-AIMv2 variant to perform well in TallyQA and CountBenchQA compared to other spatial benchmarks [17].



(a) SigLIP2 (b) AIMv2 (d) SigLIP2 (e) AIMv2
 (c) Output for prompt: *Locate the cup that contains green liquid. Provide the bounding boxes.* (f) Output for prompt: *Locate the pieces of green onions in the ramen bowl. Provide the bounding box coordinates given the size of the image is 550x550.*

Figure 4. Object localization in LLaVA-SigLIP2 vs. LLaVA-AIMv2 for different prompts.

Table 4 shows that Qwen2.5-VL achieves the strongest

Figure 3. Example image from LLaVA-Bench (In-the-Wild) [24].



Table 3. Model outputs for the prompt *Are the chopsticks to the left or right of the bowl?* on image shown in Figure 3. [24].

Model	Output
LLaVA-v1.5	The chopsticks are to the right of the bowl.
LLaVA-2D-RoPE	The chopsticks are to the right of the bowl.
LLaVA-SigLIP	The chopsticks are to the right of the bowl.
LLaVA-SigLIP-2D-RoPE	The chopsticks are to the right of the bowl.
LLaVA-SigLIP2	The chopsticks are to the right of the bowl.
LLaVA-SigLIP2-2D-RoPE	Right
LLaVA-AIMv2	The chopsticks are to the right of the bowl.
LLaVA-AIMv2-2D-RoPE	The chopsticks are to the right of the bowl.
Qwen2.5-VL	The chopsticks are to the right of the bowl.
Gemma3-4b-it	The chopsticks are to the left of the bowl.

results among frontier models on all CV-Bench 2D tasks. Among our LLaVA variants, LLaVA-AIMv2 excels in CV-Bench 2D subtasks such as COCO and ADE20K. This is because the model’s pre-training objective aligns with the nature of these tasks. COCO is for object detection and instance segmentation, and ADE20K is a scene parsing benchmark. Performance on these subtasks of CV-Bench 2D depends on the model’s ability to capture fine-grained, pixel-level representations of spatial relationships. On the other hand, CLIP and SigLIP perform less effectively on these tasks. Their core objective is to learn a global vector for image-text matching, not a dense feature map. This limitation prevents them from achieving fine-grained visual understanding. Consequently, adding 2D-RoPE only helps to organize these global-level representations from these encoders and does not enable the model to learn any dense representations. SigLIP2’s caption-based pretraining from LocCa [41] along with self-distillation and masked prediction from SILC [29] and TIPS [26] explicitly directs the model to associate language to specific and relevant regions of the image. As a result, we see that SigLIP2 performs better than its predecessor in the subtasks of CV-Bench 2D.

An interesting observation in Table 4 is that LLaVA-SigLIP2 lags behind LLaVA-AIMv2 which might be unexpected given SigLIP2’s masked image prediction objective. We think this is because the dense supervision is a secondary objective in SigLIP2. Dense supervision losses are added during the last 20% of the training in SigLIP2[40]. On the other hand, the core training objective of AIMv2 is based on learning the dense features from the very beginning. A qualitative example is shown in Figure 4 to demonstrate how LLaVA-AIMv2 is more precise in locating objects than LLaVA-SigLIP2.

As shown in Table 5, LLaVA-NeXT leads the GQA Query and Overall performance. PaliGemma leads GQA Choose and Logical. Among our trained LLaVA variants, the SigLIP-based models stand out: LLaVA-SigLIP-2D-

RoPE achieves the highest scores on Overall, Choose, Compare, and Query, while LLaVA-SigLIP2-2D-RoPE leads on Logical and Verify. LLaVA-AIMv2-2D-RoPE shows moderate improvements over its baseline, particularly on Compare and Logical, but it does not surpass the SigLIP-based variants. We observe that Gemma3-4b-it surpasses the LLaVA variants, including the 2D-RoPE variants of SigLIP and SigLIP2 for GQA Choose subtask. We think this is because how Gemma3 is trained on supervised distillation from a large teacher model with a frozen visual encoder, making it an effective classifier. The Choose subtask of GQA is a constrained multi-task classification problem that aligns well with the training benefits of Gemma3. For other GQA subtasks, LLaVA 2D-RoPE variants of SigLIP, SigLIP2, and AIMv2 surpass Gemma3. We think that the structural advantage of 2D-RoPE performs well with the object and attribute relationships like GQA Compare, Logical. For subtasks like GQA Query and Verify, the model needs to confirm information related to a specific object or attribute. SigLIP2’s self-supervised losses and masked prediction result in rich local representations that are needed for these complex, compositional reasoning.

Table 4. Comparison of frontier models and LLaVA variants on CV-Bench 2D tasks. Values underlined indicate the best-performing model overall, while values in **bold** highlight the best-performing LLaVA encoder variant in each benchmark.

Models	CV-Bench	CV-Bench	CV-Bench
	2D COCO	2D ADE20K	2D Overall
LLaVA-NeXT	0.680	0.532	0.606
LLaVA-OneVision	0.775	0.684	0.730
Qwen2.5-VL	<u>0.820</u>	<u>0.689</u>	<u>0.754</u>
SmolVLM2	0.621	0.532	0.577
Gemma3-4b-it	0.660	0.618	0.659
PaliGemma	0.675	0.573	0.624
Molmo	0.773	0.684	0.728
LLaVA-1.5	0.525	0.455	0.490
LLaVA-2D-RoPE	0.461	0.425	0.443
LLaVA-SigLIP	0.440	0.384	0.412
LLaVA-SigLIP-2D-RoPE	0.445	0.404	0.425
LLaVA-SigLIP2	0.466	0.419	0.442
LLaVA-SigLIP2-2D-RoPE	0.436	0.393	0.415
LLaVA-AIMv2	0.480	0.453	0.466
LLaVA-AIMv2-2D-RoPE	0.456	0.408	0.432

Table 5. Comparison of frontier models and LLaVA variants on GQA subtasks. Values underlined indicate the best-performing frontier model; values in **bold** indicate the best-performing LLaVA variant.

Models	GQA	GQA	GQA	GQA	GQA	GQA
	Overall	Choose	Compare	Logical	Query	Verify
LLaVA-NeXT	<u>63.786</u>	85.120	64.177	78.980	<u>49.875</u>	82.860
LLaVA-OneVision	62.140	83.880	66.893	80.588	46.069	<u>83.792</u>
Qwen2.5-VL	60.391	84.322	<u>73.854</u>	78.702	43.027	82.682
SmolVLM2	50.574	67.434	47.538	64.504	37.867	70.160
Gemma3-4b-it	31.277	61.913	16.978	19.301	25.952	45.337
PaliGemma	62.570	<u>86.802</u>	73.345	<u>81.864</u>	45.893	82.549
Molmo	55.295	78.742	52.462	65.169	41.558	77.886
LLaVA-1.5	33.225	49.690	49.576	33.500	25.702	43.206
LLaVA-2D-RoPE	34.433	41.807	54.839	48.697	22.337	50.533
LLaVA-SigLIP	25.648	17.006	47.199	44.204	15.783	39.298
LLaVA-SigLIP-2D-RoPE	38.448	55.182	59.762	55.186	23.159	57.282
LLaVA-SigLIP2	23.970	16.475	40.917	41.486	14.107	39.076
LLaVA-SigLIP2-2D-RoPE	34.560	47.121	55.688	57.959	15.298	62.211
LLaVA-AIMv2	32.541	37.998	51.783	47.421	21.440	46.403
LLaVA-AIMv2-2D-RoPE	32.342	39.858	56.876	48.974	18.663	50.178

5. Conclusion

We demonstrate that encoder choice significantly impacts spatial reasoning. For example, CountBenchQA improves about 58%, rising from 0.468 in LLaVA-1.5 to 0.739 in LLaVA-AIMv2. The effects of injecting 2D-RoPE into the image encoder attention are mixed, indicating that where and how 2D positional information is introduced matter. In our experiments, frontier models such as Qwen2.5-VL

achieve the strongest overall results. Although Qwen2.5-VL is trained on a different dataset and token scales than LLaVA, the comparison is not strictly apples-to-apples. Overall, the findings highlight that encoder design shapes spatial awareness within VLM families, although comparisons to frontier models remain questionable due to differences in training data and scale.

6. Future Work

Our study focused on static, 2D images, benchmarks and encoder variants within the LLaVA framework. This work can extend to 3D spatial reasoning along with the dynamic environment. Another potential extension can be on SigLIP2 with NaFlex. The flexible resolution image preprocessing of NaFlex mitigates information loss observed in fixed-resolution encoders. Similarly BLIP-2 and related architectures could help assess whether their pretraining objectives and visual-language alignment strategies offer advantages over CLIP-derived models. Finally, we note that advanced alignment mechanisms, such as gated attention in Flamingo [2], Q-Former in BLIP-2, or cross-modal pooling in MM1 [28], were intentionally left out in this work. Exploring these approaches as alternatives to simple projection layers may further improve spatial reasoning performance.

7. Acknowledgment

We gratefully acknowledge EleutherAI for providing GPU resources that supported this work. We also thank the volunteer team members for their time, dedication, and invaluable contributions.

References

- [1] Manoj Acharya, Kushal Kafle, and Christopher Kanan. TallyQA: Answering Complex Counting Questions. In *Proceedings of the AAAI Conference on Artificial Intelligence*, pages 8076–8084, 2019. [3](#)
- [2] Jean-Baptiste Alayrac, Jeff Donahue, Pauline Luc, Antoine Miech, Iain Barr, Yana Hasson, Karel Lenc, Arthur Mensch, Katherine Millican, Malcolm Reynolds, et al. Flamingo: a Visual Language Model for Few-Shot Learning. *Advances in Neural Information Processing Systems*, 35:23716–23736, 2022. [1, 2, 8](#)
- [3] Ahmad Mustafa Anis, Hasnain Ali, and Saquib Sarfraz. On the limitations of vision-language models in understanding image transforms, 2025. [1](#)
- [4] Shuai Bai, Keqin Chen, Xuejing Liu, Jialin Wang, Wenbin Ge, Sibo Song, Kai Dang, Peng Wang, Shijie Wang, Jun Tang, Humen Zhong, Yuanzhi Zhu, Mingkun Yang, Zhao-hai Li, Jianqiang Wan, Pengfei Wang, Wei Ding, Zheren Fu, Yiheng Xu, Jiabo Ye, Xi Zhang, Tianbao Xie, Zesen Cheng, Hang Zhang, Zhibo Yang, Haiyang Xu, and Junyang Lin. Qwen2.5-VL Technical Report, 2025. [3](#)
- [5] Lucas Beyer, Andreas Steiner, André Susano Pinto, Alexander Kolesnikov, Xiao Wang, Daniel Salz, Maxim Neumann, Ibrahim Alabdulmohsin, Michael Tschannen, Emanuele Bugliarello, Thomas Unterthiner, Daniel Keysers, Skanda Koppula, Fangyu Liu, Adam Grycner, Alexey Gritsenko, Neil Houlsby, Manoj Kumar, Keran Rong, Julian Eisenschlos, Rishabh Kabra, Matthias Bauer, Matko Bošnjak, Xi Chen, Matthias Minderer, Paul Voigtlaender, Ioana Bica, Ivana Balazevic, Joan Puigcerver, Pinelopi Papalampidi, Olivier Henaff, Xi Xiong, Radu Soricut, Jeremiah Harmsen, and Xiaohua Zhai. PaliGemma: A versatile 3B VLM for transfer. *arXiv preprint arXiv:2407.07726*, 2024. [3](#)
- [6] Boyuan Chen, Zhuo Xu, Sean Kirmani, Brian Ichter, Danny Driess, Pete Florence, Dorsa Sadigh, Leonidas Guibas, and Fei Xia. SpatialVLM: Endowing Vision-Language Models with Spatial Reasoning Capabilities, 2024. [2](#)
- [7] Xi Chen, Xiao Wang, Soravit Changpinyo, AJ Piergiovanni, Piotr Padlewski, Daniel Salz, Sebastian Goodman, Adam Grycner, Basil Mustafa, Lucas Beyer, et al. PaLI: A Jointly-Scaled Multilingual Language-Image Model. *arXiv preprint arXiv:2209.06794*, 2022. [2](#)
- [8] Xi Chen, Josip Djolonga, Piotr Padlewski, Basil Mustafa, Soravit Changpinyo, Jialin Wu, Carlos Riquelme Ruiz, Sebastian Goodman, Xiao Wang, Yi Tay, et al. PaLI-X: On Scaling up a Multilingual Vision and Language Model. *arXiv preprint arXiv:2305.18565*, 2023. [2](#)
- [9] An-Chieh Cheng, Hongxu Yin, Yang Fu, Qiushan Guo, Ruihan Yang, Jan Kautz, Xiaolong Wang, and Sifei Liu. SpatialRGPT: Grounded Spatial Reasoning in Vision Language Models, 2024. [2](#)
- [10] Federico Cocchi, Nicholas Moratelli, Davide Caffagni, Sara Sarto, Lorenzo Baraldi, Marcella Cornia, and Rita Cucchiara. LLaVA-MORE: A Comparative Study of LLMs and Visual Backbones for Enhanced Visual Instruction Tuning, 2025. [2](#)
- [11] Erik Daxberger, Nina Wenzel, David Griffiths, Haiming Gang, Justin Lazarow, Gefen Kohavi, Kai Kang, Marcin Eichner, Yinfei Yang, Afshin Dehghan, and Peter Grasch. MM-Spatial: Exploring 3D Spatial Understanding in Multimodal LLMs, 2025. [2](#)
- [12] Matt Deitke, Christopher Clark, Sangho Lee, Rohun Tripathi, Yue Yang, Jae Sung Park, Mohammadreza Salehi, Niklas Muenninghoff, Kyle Lo, Luca Soldaini, et al. Molmo and PixMo: Open Weights and Open Data for State-of-the-Art Multimodal Models. *arXiv preprint arXiv:2409.17146*, 2024. [2, 3](#)
- [13] Alexey Dosovitskiy, Lucas Beyer, Alexander Kolesnikov, Dirk Weissenborn, Xiaohua Zhai, Thomas Unterthiner, Mostafa Dehghani, Matthias Minderer, Georg Heigold, Sylvain Gelly, Jakob Uszkoreit, and Neil Houlsby. An image is worth 16x16 words: Transformers for image recognition at scale, 2021. [1](#)
- [14] Enrico Fini, Mustafa Shukor, Xiujun Li, Philipp Dufter, Michal Klein, David Haldimann, Sai Aitharaju, Victor Guilherme Turrisi da Costa, Louis Béthune, Zhe Gan, Alexander T Toshev, Marcin Eichner, Moin Nabi, Yinfei Yang, Joshua M. Susskind, and Alaaeldin El-Nouby. Multimodal autoregressive pre-training of large vision encoders, 2024. [1, 2](#)
- [15] Drew A. Hudson and Christopher D. Manning. GQA: A New Dataset for Real-World Visual Reasoning and Compositional Question Answering. In *Proceedings of the IEEE/CVF Conference on Computer Vision and Pattern Recognition (CVPR)*, pages 6700–6709, 2019. [3](#)
- [16] Jaeseok Jeong, Junho Kim, Yunjey Choi, Gayoung Lee, and Youngjung Uh. Visual style prompting with swapping self-attention, 2024. [1](#)

[17] Zhengfeng Lai, Vasileios Saveris, Chen Chen, Hong-You Chen, Haotian Zhang, Bowen Zhang, Juan Lao Tebar, Wenzhe Hu, Zhe Gan, Peter Grasch, Meng Cao, and Yinfei Yang. Revisit large-scale image-caption data in pre-training multi-modal foundation models, 2024. 5

[18] Bo Li, Yuanhan Zhang, Dong Guo, Renrui Zhang, Feng Li, Hao Zhang, Kaichen Zhang, Peiyuan Zhang, Yanwei Li, Ziwei Liu, and Chunyuan Li. LLaVA-OneVision: Easy Visual Task Transfer, 2024. 3

[19] Chengzu Li, Caiqi Zhang, Han Zhou, Nigel Collier, Anna Korhonen, and Ivan Vulić. Topviewrs: Vision-language models as top-view spatial reasoners. In *Proceedings of the 2024 Conference on Empirical Methods in Natural Language Processing*, pages 1786–1807, Miami, Florida, USA, 2024. Association for Computational Linguistics. 3

[20] Junnan Li, Dongxu Li, Caiming Xiong, and Steven Hoi. BLIP: Bootstrapping Language-Image Pre-training for Unified Vision-Language Understanding and Generation, 2022. 2

[21] Junnan Li, Dongxu Li, Silvio Savarese, and Steven Hoi. BLIP-2: Bootstrapping Language-Image Pre-training with Frozen Image Encoders and Large Language Models. In *International conference on machine learning*, pages 19730–19742. PMLR, 2023. 1, 2

[22] Fangyu Liu, Guy Emerson, and Nigel Collier. Visual Spatial Reasoning. *Transactions of the Association for Computational Linguistics*, 11:635–651, 2023. 3

[23] Haotian Liu, Chunyuan Li, Yuheng Li, and Yong Jae Lee. Improved Baselines with Visual Instruction Tuning, 2023. 2

[24] Haotian Liu, Chunyuan Li, Qingyang Wu, and Yong Jae Lee. Visual Instruction Tuning, 2023. 1, 2, 3, 6

[25] Haotian Liu, Chunyuan Li, Yuheng Li, Bo Li, Yuanhan Zhang, Sheng Shen, and Yong Jae Lee. LLaVA-NeXT: Improved reasoning, OCR, and world knowledge, 2024. 3

[26] Kevis-Kokitsi Maninis, Kaifeng Chen, Soham Ghosh, Arjun Karpur, Koert Chen, Ye Xia, Bingyi Cao, Daniel Salz, Guangxing Han, Jan Dlabař, Dan Gnanapragasam, Mojtaba Seyedhosseini, Howard Zhou, and Andre Araujo. TIPS: Text-Image Pretraining with Spatial awareness, 2025. 1, 6

[27] Andrés Marafioti, Orr Zohar, Miquel Farré, Merve Noyan, Elie Bakouch, Pedro Cuenca, Cyril Zakka, Loubna Ben Allal, Anton Lozhkov, Nouamane Tazi, Vaibhav Srivastav, Joshua Lochner, Hugo Larcher, Mathieu Morlon, Lewis Tunstall, Leandro von Werra, and Thomas Wolf. SmolVLM: Redefining small and efficient multimodal models. *arXiv preprint arXiv:2504.05299*, 2025. 3

[28] Brandon McKinzie, Zhe Gan, Jean-Philippe Fauconnier, Sam Dodge, Bowen Zhang, Philipp Dufter, Dhruti Shah, Xianzhi Du, Futang Peng, Floris Weers, et al. MM1: Methods, Analysis & Insights from Multimodal LLM Pre-training. *arXiv preprint arXiv:2403.09611*, 2024. 8

[29] Muhammad Ferjad Naeem, Yongqin Xian, Xiaohua Zhai, Lukas Hoyer, Luc Van Gool, and Federico Tombari. SILC: Improving Vision Language Pretraining with Self-Distillation, 2023. 6

[30] Maxime Oquab, Timothée Darcet, Théo Moutakanni, Huy Vo, Marc Szafraniec, Vasil Khalidov, Pierre Fernandez, Daniel Haziza, Francisco Massa, Alaaeldin El-Nouby, Mahmoud Assran, Nicolas Ballas, Wojciech Galuba, Russell Howes, Po-Yao Huang, Shang-Wen Li, Ishan Misra, Michael Rabbat, Vasu Sharma, Gabriel Synnaeve, Hu Xu, Hervé Jegou, Julien Mairal, Patrick Labatut, Armand Joulin, and Piotr Bojanowski. DINOv2: Learning Robust Visual Features without Supervision, 2024. 1, 2

[31] Xichen Pan, Li Dong, Shaohan Huang, Zhiliang Peng, Wenhui Chen, and Furu Wei. Kosmos-G: Generating Images in Context with Multimodal Large Language Models. *ArXiv*, abs/2310.02992, 2023. 2

[32] Zhiliang Peng, Wenhui Wang, Li Dong, Yaru Hao, Shaohan Huang, Shuming Ma, and Furu Wei. Kosmos-2: Grounding Multimodal Large Language Models to the World. *arXiv preprint arXiv:2306.14824*, 2023. 2

[33] Alec Radford, Jong Wook Kim, Chris Hallacy, Aditya Ramesh, Gabriel Goh, Sandhini Agarwal, Girish Sastry, Amanda Askell, Pamela Mishkin, Jack Clark, et al. Learning Transferable Visual Models From Natural Language Supervision. In *International conference on machine learning*, pages 8748–8763. PMLR, 2021. 1, 2

[34] Chan Hee Song, Valts Blukis, Jonathan Tremblay, Stephen Tyree, Yu Su, and Stan Birchfield. Robospatial: Teaching spatial understanding to 2d and 3d vision-language models for robotics, 2025. 2

[35] Jianlin Su, Yu Lu, Shengfeng Pan, Ahmed Murtadha, Bo Wen, and Yunfeng Liu. Roformer: Enhanced transformer with rotary position embedding, 2023. 1

[36] Quan Sun, Yuxin Fang, Ledell Wu, Xinlong Wang, and Yue Cao. Eva-clip: Improved training techniques for clip at scale, 2023. 1

[37] Gemma Team, Aishwarya Kamath, Johan Ferret, Shreya Pathak, Nino Vieillard, Ramona Merhej, Sarah Perrin, Tatiana Matejovicova, Alexandre Ramé, Morgane Rivière, Louis Rouillard, Thomas Mesnard, Geoffrey Cideron, Jean bastien Grill, Sabela Ramos, Edouard Yvinec, Michelle Casbon, Etienne Pot, Ivo Penchev, Gaël Liu, Francesco Visin, Kathleen Kenealy, Lucas Beyer, Xiaohai Zhai, Anton Tsitsulin, Robert Busa-Fekete, Alex Feng, Noveen Sachdeva, Benjamin Coleman, Yi Gao, Basil Mustafa, Iain Barr, Emilio Parisotto, David Tian, Matan Eyal, Colin Cherry, Jan-Thorsten Peter, Danila Sinopalnikov, Surya Bhupatiraju, Rishabh Agarwal, Mehran Kazemi, Dan Malkin, Ravin Kumar, David Vilar, Idan Brusilovsky, Jiaming Luo, Andreas Steiner, Abe Friesen, Abhanshu Sharma, Abheesh Sharma, Adi Mayrav Gilady, Adrian Goedekemeyer, Alaa Saade, Alex Feng, Alexander Kolesnikov, Alexei Bendebury, Alvin Abdagic, Amit Vadi, András György, André Susano Pinto, Anil Das, Ankur Bapna, Antoine Miech, Antoine Yang, Antonia Paterson, Ashish Shenoy, Ayan Chakrabarti, Bilal Piot, Bo Wu, Bobak Shahriari, Bryce Petrini, Charlie Chen, Charline Le Lan, Christopher A. Choquette-Choo, CJ Carey, Cormac Brick, Daniel Deutsch, Danielle Eisenbud, Dee Castle, Derek Cheng, Dimitris Paparas, Divyashree Shivakumar Sreepathihalli, Doug Reid, Dustin Tran, Dustin Zelle, Eric Noland, Erwin Huizinga, Eugene Kharitonov, Frederick Liu, Gagik Amirkhanyan, Glenn Cameron, Hadi Hashemi, Hanna Klimczak-Plucińska, Harman Singh, Harsh Mehta,

Harshal Tushar Lehri, Hussein Hazimeh, Ian Ballantyne, Idan Szpektor, Ivan Nardini, Jean Pouget-Abadie, Jetha Chan, Joe Stanton, John Wieting, Jonathan Lai, Jordi Orabay, Joseph Fernandez, Josh Newlan, Ju yeong Ji, Jyotinder Singh, Kat Black, Kathy Yu, Kevin Hui, Kiran Vodrahalli, Klaus Greff, Linhai Qiu, Marcella Valentine, Marina Coelho, Marvin Ritter, Matt Hoffman, Matthew Watson, Mayank Chaturvedi, Michael Moynihan, Min Ma, Nabila Babar, Natasha Noy, Nathan Byrd, Nick Roy, Nikola Momichev, Nilay Chauhan, Noveen Sachdeva, Oskar Bunyan, Pankil Botarda, Paul Caron, Paul Kishan Rubenstein, Phil Culliton, Philipp Schmid, Pier Giuseppe Sessa, Pingmei Xu, Piotr Stanczyk, Pouya Tafti, Rakesh Shivanna, Renjie Wu, Renke Pan, Reza Rokni, Rob Willoughby, Rohith Vallu, Ryan Mullins, Sammy Jerome, Sara Smoot, Sertan Girgin, Shariq Iqbal, Shashir Reddy, Shruti Sheth, Siim Põder, Sijal Bhatnagar, Sindhu Raghuvaran Panyam, Sivan Eiger, Susan Zhang, Tianqi Liu, Trevor Yacovone, Tyler Liechty, Uday Kalra, Utku Evcı, Vedant Misra, Vincent Roseberry, Vlad Feinberg, Vlad Kolesnikov, Woohyun Han, Woosuk Kwon, Xi Chen, Yinlam Chow, Yuvein Zhu, Zichuan Wei, Zoltan Egyed, Victor Cotruta, Minh Giang, Phoebe Kirk, Anand Rao, Kat Black, Nabila Babar, Jessica Lo, Erica Moreira, Luiz Gustavo Martins, Omar Sanseviero, Lucas Gonzalez, Zach Gleicher, Tris Warkentin, Vahab Mirrokni, Evan Senter, Eli Collins, Joelle Barral, Zoubin Ghahramani, Raia Hadsell, Yossi Matias, D. Sculley, Slav Petrov, Noah Fiedel, Noam Shazeer, Oriol Vinyals, Jeff Dean, Demis Hassabis, Koray Kavukcuoglu, Clement Farabet, Elena Buchatskaya, Jean-Baptiste Alayrac, Rohan Anil, Dmitry Lepikhin, Sebastian Borgeaud, Olivier Bachem, Armand Joulin, Alek Andreev, Cassidy Hardin, Robert Dadashi, and Léonard Hussenot. Gemma 3 technical report, 2025. [3](#)

[38] Shengbang Tong, Ellis Brown, Penghao Wu, Sanghyun Woo, Manoj Middepogu, Sai Charitha Akula, Jihan Yang, Shusheng Yang, Adithya Iyer, Xichen Pan, Austin Wang, Rob Fergus, Yann LeCun, and Saining Xie. Cambrian-1: A Fully Open, Vision-Centric Exploration of Multimodal LLMs. In *Advances in Neural Information Processing Systems*, 2024. [3](#)

[39] Shengbang Tong, Zhuang Liu, Yuexiang Zhai, Yi Ma, Yann LeCun, and Saining Xie. Eyes wide shut? exploring the visual shortcomings of multimodal llms, 2024. [1, 3](#)

[40] Michael Tschannen, Alexey Gritsenko, Xiao Wang, Muhammad Ferjad Naeem, Ibrahim Alabdulmohsin, Nikhil Parthasarathy, Talfan Evans, Lucas Beyer, Ye Xia, Basil Mustafa, Olivier Hénaff, Jeremiah Harmsen, Andreas Steiner, and Xiaohua Zhai. SigLIP 2: Multilingual Vision-Language Encoders with Improved Semantic Understanding, Localization, and Dense Features, 2025. [1, 2, 6](#)

[41] Bo Wan, Michael Tschannen, Yongqin Xian, Filip Pavetic, Ibrahim Alabdulmohsin, Xiao Wang, André Susano Pinto, Andreas Steiner, Lucas Beyer, and Xiaohua Zhai. Locca: Visual pretraining with location-aware captioners, 2024. [6](#)

[42] Peng Wang, Shuai Bai, Sinan Tan, Shijie Wang, Zhihao Fan, Jinze Bai, Keqin Chen, Xuejing Liu, Jialin Wang, Wenbin Ge, et al. Qwen2-VL: Enhancing Vision-Language Model's Perception of the World at Any Resolution. *arXiv preprint arXiv:2409.12191*, 2024. [1, 2](#)

[43] Bin Xiao, Haiping Wu, Weijian Xu, Xiyang Dai, Houdong Hu, Yumao Lu, Michael Zeng, Ce Liu, and Lu Yuan. Florence-2: Advancing a unified representation for a variety of vision tasks. In *Proceedings of the IEEE/CVF Conference on Computer Vision and Pattern Recognition*, pages 4818–4829, 2024. [1, 2](#)

[44] Xiaohua Zhai, Basil Mustafa, Alexander Kolesnikov, and Lucas Beyer. Sigmoid Loss for Language Image Pre-Training. In *Proceedings of the IEEE/CVF International Conference on Computer Vision*, pages 11975–11986, 2023. [2](#)

[45] Huanyu Zhang, Chengzu Li, Wenshan Wu, Shaoguang Mao, Yifan Zhang, Haochen Tian, Ivan Vulić, Zhang Zhang, Liang Wang, Tieniu Tan, and Furu Wei. Scaling and beyond: Advancing spatial reasoning in mllms requires new recipes, 2025. [1, 2](#)

[46] Wanyue Zhang, Yibin Huang, Yangbin Xu, JingJing Huang, Helu Zhi, Shuo Ren, Wang Xu, and Jiajun Zhang. Why do mllms struggle with spatial understanding? a systematic analysis from data to architecture, 2025. [1](#)